

Fluxtube dynamics in neutron star cores

- Implications for magnetic field evolution

SMFNS2017
Varadero, Cuba

Vanessa Graber, McGill University
vanessa.graber@mcgill.ca



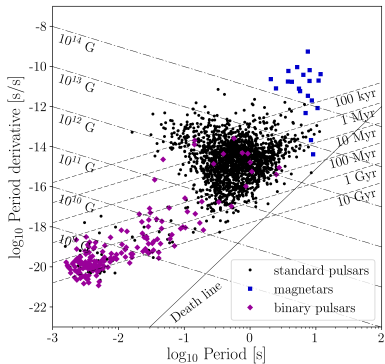


Figure 1: Neutron star $P\dot{P}$ diagram.

- Inferred magnetic dipole field strengths reach up to 10^{15} G for magnetars. Such fields strongly influence the stars' dynamics.
- Long-term **field evolution** could explain
 - ▶ observed field changes in pulsars
 - ▶ high activity of magnetars
 - ▶ neutron star 'metamorphosis'
- Mechanisms causing magnetic field evolution are poorly understood.

What happens if we account for core superconductivity?

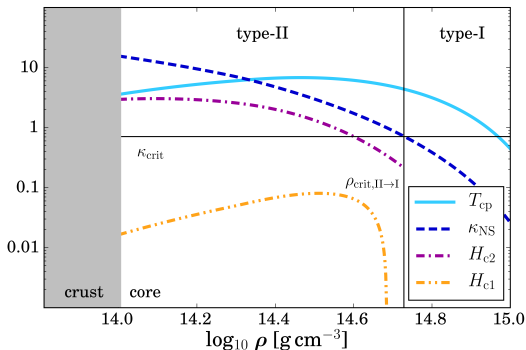
- Equilibrium stars have $10^6 - 10^8$ K, while for nucleons $T_F \sim 10^{12}$ K \Rightarrow they are cold enough to contain **superfluid** neutrons and **superconducting** protons. Cooper pair formation occurs due to an **attractive contribution** to the nucleon-nucleon interaction.
- The type of superconductivity depends on the characteristic lengthscales. Estimates predict a **type-II state** (Baym, Pethick & Pines, 1969b; Mendell, 1991)

$$\kappa_{\text{NS}} = \frac{\lambda}{\xi_{\text{ft}}} \approx 3 \left(\frac{m_{\text{p}}^*}{m} \right)^{\frac{3}{2}} \rho_{14}^{-\frac{5}{6}} \left(\frac{x_{\text{p}}}{0.05} \right)^{-\frac{5}{6}} \left(\frac{T_{\text{cp}}}{10^9 \text{ K}} \right) > \frac{1}{\sqrt{2}}, \quad (1)$$

$$H_{\text{c1}} = \frac{4\pi\mathcal{E}_{\text{ft}}}{\phi_0} \approx 1.9 \times 10^{14} \left(\frac{m}{m_{\text{p}}^*} \right) \rho_{14} \left(\frac{x_{\text{p}}}{0.05} \right) \text{ G}, \quad (2)$$

$$H_{\text{c2}} = \frac{\phi_0}{2\pi\xi_{\text{ft}}^2} \approx 2.1 \times 10^{15} \left(\frac{m_{\text{p}}^*}{m} \right)^2 \rho_{14}^{-\frac{2}{3}} \left(\frac{x_{\text{p}}}{0.05} \right)^{-\frac{2}{3}} \left(\frac{T_{\text{cp}}}{10^9 \text{ K}} \right)^2 \text{ G}. \quad (3)$$

Figure 2: Density-dependent parameters of NS superconductivity calculated for the NRAPR effective equation of state (Steiner et al., 2005).



Shown are κ_{NS} , T_{cp} (normalised to 10^9 K), H_{c2} and H_{c1} (normalised to 10^{16} G). The horizontal and vertical line mark $\kappa_{crit} = 1/\sqrt{2}$ and $\rho_{crit,II \rightarrow I}$, respectively.

- Magnetic flux enters the system in the form of **quantised fluxtubes**, arranged in a hexagonal array. Each fluxtube carries a unit of flux,

$$\phi_0 = \frac{hc}{2e} \approx 2 \times 10^{-7} \text{ G cm}^2. \quad (4)$$

- All flux quanta add up to the macroscopic magnetic induction B in the star's core.
- Relate B to the fluxtube surface density and interfluxtube distance:

$$\mathcal{N}_{\text{ft}} = \frac{B}{\phi_0} \approx 4.8 \times 10^{18} B_{12} \text{ cm}^{-2}, \quad d_{\text{ft}} \simeq \mathcal{N}_{\text{ft}}^{-\frac{1}{2}} \approx 4.6 \times 10^{-10} B_{12}^{-\frac{1}{2}} \text{ cm}. \quad (5)$$

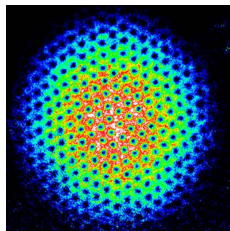


Figure 3: Vortex array in a rotating BEC (Engels et al., 2002).

Magnetic field evolution is linked to the motion of fluxtubes!

- Matter **inside fluxtubes** is normal conducting \Rightarrow the dominant coupling is scattering of electrons off normal protons (Baym, Pethick & Pines, 1969a). This process is characterised by an **electrical conductivity**

$$\sigma_e = \frac{n_e e^2 c \tau}{\hbar k_{\text{Fe}}} \approx 5.5 \times 10^{28} T_8^{-2} \rho_{14}^{\frac{3}{2}} \left(\frac{x_p}{0.05} \right)^{\frac{3}{2}} \text{ s}^{-1}. \quad (6)$$

- Relate this to **standard Ohmic diffusion**

$$\tau_{\text{Ohm}} = \frac{4\pi\sigma_e L^2}{c^2} \approx 2.5 \times 10^{13} T_8^{-2} L_6^2 \rho_{14}^{\frac{3}{2}} \left(\frac{x_p}{0.05} \right)^{\frac{3}{2}} \text{ yr}. \quad (7)$$

- Timescales are very long and further lengthened as fluxtubes only occupy a small fraction of the star's volume, estimated as $B/H_{c2} \sim 10^{-3} B_{12}$.

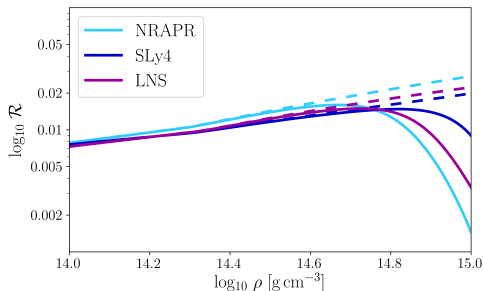
- Fluxtubes are magnetised \Rightarrow electrons can scatter off this magnetic field (Alpar, Langer & Sauls, 1984). In analogy with superfluid hydrodynamics this is generally called **mutual friction**: $\mathbf{f}_d = \rho_p \kappa \mathcal{R} (\mathbf{v}_e - \mathbf{v}_{ft})$.
- Using the formalism of Sauls, Stein & Serene (1982) it is possible to determine the corresponding, **dimensionless drag coefficient**. For typical neutron star parameters we obtain

$$\mathcal{R} = \frac{1}{\mathcal{N}_{ft} \kappa} \frac{E_{Fe}}{mc^2} \frac{1}{\tau} \approx 1.6 \times 10^{-2} B_{12}^{-1} \left(\frac{k_{Fe}}{0.75 \text{ fm}^{-1}} \right) \left(\frac{10^{-15} \text{ s}}{\tau} \right) \ll 1. \quad (8)$$

- Since $\mathcal{R} \ll 1$, this is referred to as the limit of weak mutual friction.

For a given EoS and superconducting gap model, \mathcal{R} can be calculated as a function of the star's density.

- Resistive drag coefficients for three different EoS (Chamel, 2008) and a standard proton gap parametrisation (Ho, Glampedakis & Andersson, 2012).



- Approximate solution often found in the literature is independent of Δ :

$$\mathcal{R} \approx \frac{3\pi^2}{64} \frac{1}{\lambda k_{\text{Fe}}} \approx 7.9 \times 10^{-3} \left(\frac{m}{m_p^*} \right)^{1/2} \rho_{14}^{1/6} \left(\frac{x_p}{0.05} \right)^{1/6}. \quad (9)$$

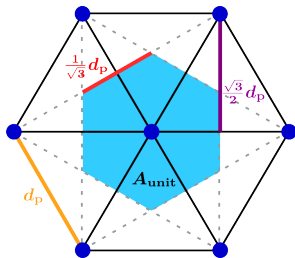
- Deriving a **superconducting induction equation** it can be shown that this mechanism can also not drive fast field evolution (Graber et al., 2015).

- Two parallel fluxtubes separated by r_{21} experience a **repulsive force** per unit length

$$\mathbf{F}_{12} = -\nabla\mathcal{E}_{\text{int}} = -\frac{\phi_0^2}{8\pi^2\lambda^3} K_1\left(\frac{r_{21}}{\lambda}\right) \hat{\mathbf{r}}_{21}. \quad (10)$$

- For a **lattice**, the net force on a single line is obtained by summing individual contributions.
- In the **triangular case** all terms cancel and no field changes takes place.
- However, in a realistic fluxtube lattice the long-range order is likely to be destroyed \Rightarrow a **gradient** in \mathcal{N}_{ft} results in a non-zero net force on the fluxtubes, which would drive field evolution. We expect

$$\mathbf{F}_{\text{rep}} = -g(\mathcal{N}_{\text{ft}})\nabla\mathcal{N}_{\text{ft}}. \quad (11)$$



- For standard pulsars with $10^{12} - 10^{13}$ G the problem simplifies because of the hierarchy of the important **lengthscales**, specifically $d_{\text{ft}} \simeq r_{21} \gg \lambda$:
 - ▶ $K_1(r_{21}/\lambda)$ can be approximated as a decaying exponential.
 - ▶ In the summation only account for the six nearest neighbours.

- In this case, we derive the following **repulsive force**

$$\mathbf{F}_{\text{rep}} \simeq -\frac{3\phi_0^2}{32\sqrt{2}\pi^{3/2}} \left(\frac{\sqrt{2}\mathcal{N}_{\text{ft}}^{-1/2}}{3^{1/4}\lambda} \right)^{\frac{7}{2}} \exp \left[-\frac{\sqrt{2}\mathcal{N}_{\text{ft}}^{-1/2}}{3^{1/4}\lambda} \right] \nabla \mathcal{N}_{\text{ft}}. \quad (12)$$

- Neglecting fluxtube inertia, the **force balance** reads

$$\sum \mathbf{f} = -g(\mathcal{N}_{\text{ft}})\nabla \mathcal{N}_{\text{ft}} - \rho_p \kappa \mathcal{R} \mathbf{v}_{\text{ft}} = 0, \quad (13)$$

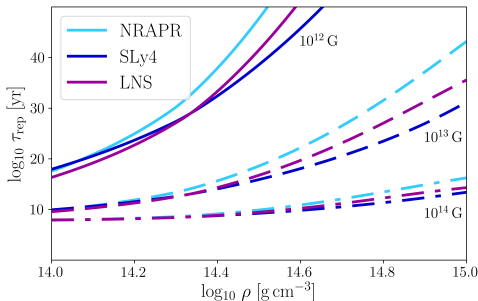
- Combine the force balance with a continuity equation for \mathcal{N}_{ft} to obtain a **non-linear diffusion equation** for the evolution of the fluxtubes/field

$$\partial_t \mathcal{N}_{\text{ft}} + \nabla (\mathcal{N}_{\text{ft}} \mathbf{u}_{\text{ft}}) = \partial_t \mathcal{N}_{\text{ft}} - \nabla \left(\frac{\mathcal{N}_{\text{ft}} g(\mathcal{N}_{\text{ft}})}{\rho_p \kappa \mathcal{R}} \nabla \mathcal{N}_{\text{ft}} \right) = 0. \quad (14)$$

- Extract a timescale for a characteristic lengthscale L :

$$\tau_{\text{rep}} = \frac{L^2 \rho_p \kappa \mathcal{R}}{\mathcal{N}_{\text{ft}} g(\mathcal{N}_{\text{ft}})}. \quad (15)$$

- Estimates for $L = 10^6$ cm and different B fields show strong variability with density.



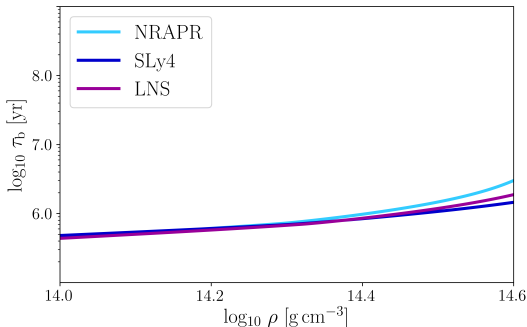
- Fluxtubes are buoyant as a result of the **magnetic pressure** inside their cores. This creates a radially acting lift force, f_b , trying to drive fluxtubes out of the core (Muslimov & Tsygan, 1985; Harvey, Ruderman & Shaham, 1986).
- The **buoyancy force** is related to the gradient of the superconducting magnetic pressure. In the limit $B \lesssim H_{c1}$, which approximates the neutron star core, one has $P = H_{c1} B / 4\pi$ (Easson & Pethick, 1977). This gives

$$f_b = \frac{|-\nabla P|}{\mathcal{N}_{ft}} \simeq \frac{H_{c1} B}{\mathcal{N}_{ft} 4\pi L} = \frac{H_{c1} \phi_0}{4\pi L} = \frac{\phi_0^2}{16\pi^2 \lambda^2 L} \ln\left(\frac{\lambda}{\xi_{ft}}\right). \quad (16)$$

- Balancing the resistive drag with the buoyancy force, we arrive at a similar non-linear diffusion equation. The respective **timescale** reads

$$\tau_b = L^2 \rho_p \kappa \mathcal{R} \frac{16\pi^2 \lambda^2}{\phi_0^2 \ln(\lambda/\xi_{ft})}. \quad (17)$$

- Estimates for $L = 10^6$ cm are of the order of observed field changes.



- Self-consistent **magneto-thermal simulations** of superconducting cores show that buoyancy is too weak to drive field evolution (Elfritz et al., 2016).

Conclusions

- We have studied various mechanisms that are expected to affect the **superconducting fluxtubes** present in the outer neutron star core and calculated characteristic timescales for **realistic equations of state**.
- Resulting field changes act on shortest timescales at low densities, close to the crust-core interface, but are still **too long** to explain observations.
- Many **open problems** remain:
 - ▶ How do fluxtubes interact with neutron vortices?
 - ▶ Is the outer core in a type-II state after all (maybe type-I)?
 - ▶ What is the field configuration right before the phase transition?
- One **possible approach**: Use the **analogy with laboratory systems** to make progress (Graber, Andersson & Hogg, 2017).

Thank you!

Appendix

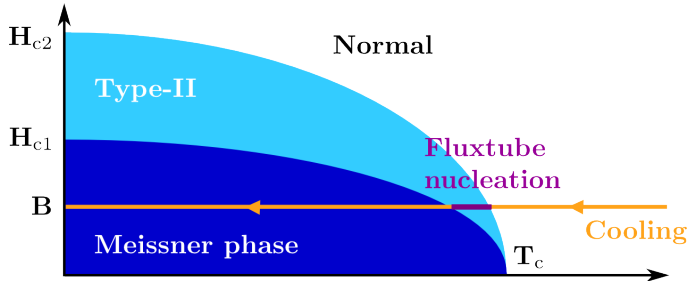


Figure 4: $H(T)$ -diagram of a type-II superconductor illustrating the phase transition. As the medium permeated by the induction $B < H_{c1}$ is cooled down, it follows the yellow line from right to left. Below the transition temperature, T_c , magnetic flux (continuously distributed in the normal state) is first nucleated into fluxtubes. These are subsequently expelled if the matter is cooled further and a flux-free Meissner state is formed.

Appendix

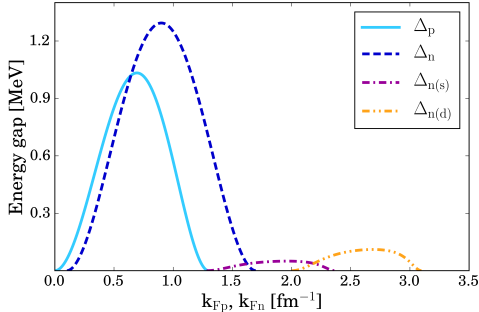


Figure 5: Parametrised energy gaps shown as a function of the proton and neutron Fermi wave numbers, k_{Fp} and k_{Fn} , respectively. Singlet-paired gaps for the protons (cyan, solid) and neutrons (blue, dashed) are found on the left. Further on the right, two different neutron triplet gaps are given, i.e. a shallow (purple, dot-dashed) and a deep (yellow, dot-dot-dashed) model.

$$\Delta(k_{Fx}) = \Delta_0 \frac{(k_{Fx} - g_0)^2}{(k_{Fx} - g_0)^2 + g_1} \frac{(k_{Fx} - g_2)^2}{(k_{Fx} - g_2)^2 + g_3}. \quad (18)$$

References

- Alpar M. A., Langer S. A., Sauls J. A., 1984, *The Astrophysical Journal*, 282, 533
- Baym G., Pethick C. J., Pines D., 1969a, *Nature*, 224, 674
- Baym G., Pethick C. J., Pines D., 1969b, *Nature*, 224, 673
- Chamel N., 2008, *Monthly Notices of the Royal Astronomical Society*, 388, 737
- Easson I., Pethick C. J., 1977, *Physical Review D*, 16, 275
- Elfritz J. G., Pons J. A., Rea N., Glampedakis K., Viganò D., 2016, *Monthly Notices of the Royal Astronomical Society*, 456, 4461
- Engels P., Coddington I., Haljan P. C., Cornell E. A., 2002, *Physical review letters*, 89, 100403
- Graber V., Andersson N., Glampedakis K., Lander S. K., 2015, *Monthly Notices of the Royal Astronomical Society*, 453, 671
- Graber V., Andersson N., Hogg M., 2017, *arXiv preprint*
- Harvey J., Ruderman M., Shaham J., 1986, *Physical Review D*, 33, 2084
- Ho W. C. G., Glampedakis K., Andersson N., 2012, *Monthly Notices of the Royal Astronomical Society*, 422, 2632
- Mendell G., 1991, *The Astrophysical Journal*, 380, 515
- Muslimov A. G., Tsygan A. I., 1985, *Soviet Astronomy Letters*, 11, 80
- Sauls J. A., Stein D. L., Serene J. W., 1982, *Physical Review D*, 25, 967
- Steiner A. W., Prakash M., Lattimer J. M., Ellis P. J., 2005, *Physics reports*, 411, 325